# Tumor Cell–Derived and Macrophage-Derived Cathepsin B Promotes Progression and Lung Metastasis of Mammary Cancer

Olga Vasiljeva,[1] Anna Papazoglou,[1] Achim Krüger,[3] Harald Brodoefel,[1] Matvey Korovin,[1] Jan Deussing,[1] Nicole Augustin,[2] Boye S. Nielsen,[4] Kasper Almholt,[4] Matthew Bogyo,[5] Christoph Peters,[1] and Thomas Reinheckel[1]

[1]Institut für Molekulare Medizin und Zellforschung and [2]Institut für Biometrie und Medizinische Informatik, Albert-Ludwigs-Universität Freiburg, Freiburg, Germany; [3]Klinikum rechts der Isar der Technischen Universität München, Institut für Experimentelle Onkologie und Therapieforschung, Munich, Germany; [4]Finsen Laboratory, Rigshospitalet, Copenhagen, Denmark; and [5]Departments of Pathology, Microbiology, and Immunology, Stanford University School of Medicine, Stanford, California

## Abstract

**Proteolysis in close vicinity of tumor cells is a hallmark of cancer invasion and metastasis. We show here that mouse mammary tumor virus–polyoma middle T antigen (PyMT) transgenic mice deficient for the cysteine protease cathepsin B (CTSB) exhibited a significantly delayed onset and reduced growth rate of mammary cancers compared with wild-type PyMT mice. Lung metastasis volumes were significantly reduced in *PyMT;ctsb*$^{+/-}$, an effect that was not further enhanced in *PyMT;ctsb*$^{-/-}$ mice. Furthermore, lung colonization studies of PyMT cells with different CTSB genotypes injected into congenic wild-type mice and *in vitro* Matrigel invasion assays confirmed a specific role for tumor-derived CTSB in invasion and metastasis. Interestingly, cell surface labeling of cysteine cathepsins by the active site probe DCG-04 detected up-regulation of cathepsin X on *PyMT;ctsb*$^{-/-}$ cells. Treatment of cells with a neutralizing anti-cathepsin X antibody significantly reduced Matrigel invasion of *PyMT;ctsb*$^{-/-}$ cells but did not affect invasion of *PyMT;ctsb*$^{+/+}$ or *PyMT;ctsb*$^{+/-}$ cells, indicating a compensatory function of cathepsin X in CTSB-deficient tumor cells. Finally, an adoptive transfer model, in which *ctsb*$^{+/+}$, *ctsb*$^{+/-}$, and *ctsb*$^{-/-}$ recipient mice were challenged with *PyMT;ctsb*$^{+/+}$ cells, was used to address the role of stroma-derived CTSB in lung metastasis formation. Notably, *ctsb*$^{-/-}$ mice showed reduced number and volume of lung colonies, and infiltrating macrophages showed a strongly up-regulated expression of CTSB within metastatic cell populations. These results indicate that both cancer cell–derived and stroma cell–derived (i.e., macrophages) CTSB plays an important role in tumor progression and metastasis.** (Cancer Res 2006; 66(10): 5242-50)

## Introduction

Invasion and metastasis of cancer result from several interdependent processes in which proteolytic enzymes have been implicated (1). Among other tumor-related features, release of tumor-derived proteases is thought to facilitate the breakdown of basement membranes and extracellular matrix (ECM), thereby promoting cancer cell invasion into surrounding normal tissues. The proteolytic enzymes implicated in tumor progression and metastasis belong to four major catalytic classes of proteases: metalloproteinases [soluble and integral membrane matrix metalloproteinases (MMP), adamalysin-related disintegrin and metalloproteinases (ADAMS), or bone morphogenetic protein-1-type proteases], serine proteases, and cysteine- and aspartyl-type lysosomal proteases (2–4). Lysosomal cysteine proteases belong to the family of papain-like proteolytic enzymes (clan CA, family C1) principally localized subcellularly in the endosomal/lysosomal compartment. Seven of these proteases, cathepsins B (CTSB), C (dipeptidyl peptidase I), F, H, L, O, and X (alternative names: cathepsin Z; cathepsin P), exhibit ubiquitous but, nevertheless, differential expression in mammalian tissues, whereas other papain-like cysteine proteases (i.e., cathepsins J, K, S, V, and W) are only expressed by specific cell types (5, 6). Traditionally, lysosomal cysteine proteases are considered to execute nonspecific bulk proteolysis within the lysosomes (7). Yet, there is growing evidence for specific functions of these enzymes (8–11). Lysosomal proteases are secreted in significant quantities to function extracellularly in certain pathologic conditions and cancer (12). Most notably, early investigations identified CTSB as highly expressed in human breast carcinomas at the invasive fronts of tumors (13).

Furthermore, increased expression and proteolytic activity of lysosomal proteases (e.g., the aspartyl proteases cathepsin D and the cysteine proteases CTSB and cathepsin L) have often been positively correlated with poor prognosis for patients with a variety of malignancies, including mammary adenocarcinomas (14–17). The majority of experimental evidence for the involvement of lysosomal cysteine proteases in tumorigenesis has been obtained using *ex vivo* culture models (18–20). Recently, a study using a broad-spectrum inhibitor for cysteine cathepsins in the Rip1-Tag2 mouse model identified roles for cysteine cathepsins in angiogenesis and tumor growth and invasiveness within pancreatic islet tumors (21). Although these studies clearly confirm the importance of this class of proteases, they have not provided specific roles for CTSB in the progression and metastasis of cancer *in vivo*.

To address the role of CTSB in cancer growth and metastasis, we established a mouse mammary cancer model in the absence of

**Note:** Supplementary data for this article are available at Cancer Research Online (http://cancerres.aacrjournals.org/).

O. Vasiljeva and A. Papazoglou contributed equally to this work. O. Vasiljeva is currently at the Department of Biochemistry and Molecular Biology, Jozef Stefan Institute, Ljubljana, Slovenia. A. Papazoglou is currently at the Department of Stereotactic Neurosurgery, University Hospital Freiburg, Freiburg, Germany. J. Deussing is currently at the Max-Planck-Institut für Psychiatrie, Molekulare Neurogenetik, Munich, Germany. N. Augustin is currently at the Department of Mathematical Sciences, University of Bath, Bath, United Kingdom.

**Requests for reprints:** Thomas Reinheckel, Institut für Molekulare Medizin und Zellforschung, Albert-Ludwigs-Universität Freiburg, Stefan Meier Strasse 17, D-79104 Freiburg, Germany. Phone: 49-761-203-9606; Fax: 49-761-203-9634; E-mail: Thomas.Reinheckel@uniklinik-freiburg.de.



doi:10.1158/0008-5472.CAN-05-4463

CTSB by crossing CTSB-deficient mice (22) with a mammary cancer-susceptible strain of mice [polyoma middle T antigen (PyMT) mice], in which the expression of the PyMT is directed to the mammary epithelium by the mouse mammary tumor virus (MMTV)-long terminal repeat (23). Here, we show a major effect of CTSB on the progression of PyMT-induced mammary carcinomas and the formation of lung metastases. Furthermore, the findings indicate a substantial contribution of CTSB from cancer cells as well as from cells of the tumor microenvironment to the growth of experimental lung metastases.

## Materials and Methods

**Animals.** To reduce the genetic background influence as a variable in the experiment, CTSB-deficient mice (22) were backcrossed for seven generations to the transgenic mouse strain FVB/N-TgN(MMTVPyVT)634-Mul (PyMT; ref. 23), which was obtained from The Jackson Laboratory (Bar Harbor, ME). After the intercross, tumor mice being wild-type, heterozygous, and deficient for CTSB have been named *PyMT;ctsb*$^{+/+}$, *PyMT;ctsb*$^{+/-}$, and *PyMT;ctsb*$^{-/-}$, respectively.

**Tumor progression study.** Beginning at age 30 days, female mice were examined thrice a week for the development of mammary tumors by finger palpation in a genotype-blinded fashion. After tumors were first detected, diameters of tumors were measured with calipers every 2nd day until age 98 days. For the male tumor progression study, mice were palpated twice a week.

**Histomorphometry.** For volumetric measurement of total lung metastases or disseminated tumor colonies in lungs, the cryoembedded lungs were cut transversally to the trachea into systematic random 2-mm-thick slabs. The 5 to 7 slabs obtained from each lung were embedded with Tissue-Tek into a single block as specified previously (24). From each block, 5 μm cryostat sections were obtained and stained with H&E. Stereologic determination of the metastasis volumes was done by computer-assisted point counting as described previously (24).

**Immunohistochemistry and immunofluorescence.** Goat anti-rat CTSB antibody (provided by E. Weber, Martin-Luther-University, Halle, Germany; ref. 22) has been used for the detection of CTSB. For CTSB-F4/80 double-label immunofluorescence microscopy, the goat anti-rat CTSB antibody was visualized by Alexa Fluor 488 donkey anti-goat antibody (Invitrogen Molecular Probes, Karlsruhe, Germany). After blocking with goat IgG, the F4/80 macrophage antigen was detected by the rat anti-mouse F4/80 antibody (Serotec, Dusseldorf, Germany) followed by Alexa Fluor 546–labeled goat anti-rat antibody (Invitrogen Molecular Probes). Nuclear staining was done with Hoechst 33342.

**Isolation of primary tumor cells from PyMT-induced mammary carcinomas.** Primary PyMT tumor cells were obtained by mechanical and enzymatic dissociation of solid PyMT-induced carcinomas. The obtained suspension was sequentially transferred through 100 and 40 μm cell strainers, washed twice with PBS, and cultured for 12 hours. Immunodetection with a pan-cytokeratin antibody (Sigma, Hamburg, Germany) revealed 98% of cytokeratin-positive tumor cells after 12 hours in culture. Vital and adherent cells were harvested by trypsinization, PBS washed, and immediately frozen in medium containing 10% DMSO for further use.

**Lung colonization assay following i.v. injection of LacZ-tagged PyMT tumor cells.** Isolated primary tumor cells were genetically tagged by retroviral transduction of the bacterial *LacZ* gene according to the manufacturer's instructions (BioCarta, Ann Arbor, MI; ref. 25). *LacZ* tagging was verified by X-gal staining, and only pools with 100% transduction efficacy were used for the assay. Two days after transduction, $1 \times 10^5$ *LacZ*-tagged primary tumor cells of the genotypes *PyMT;ctsb*$^{+/+}$, *PyMT;ctsb*$^{+/-}$, or *PyMT;ctsb*$^{-/-}$ (four donor mice per genotype) were inoculated i.v. into the tail veins of *ctsb*$^{+/+}$, *ctsb*$^{+/-}$, and *ctsb*$^{-/-}$ congenic recipient mice (five recipients per donor). Twenty-one days after tumor cell inoculation, lungs were isolated and stained with X-gal, and the number of surface colonies on the lungs were quantified.

***In vitro* cell invasion assay.** Cell culture inserts sealed by an 8-μm pore-size microporous membrane filled with Matrigel (BD Biosciences, Heidelberg, Germany) were used for invasion studies. The Matrigel was dried in a laminar hood and reconstituted with 500 μL DMEM for 1 hour at 37°C. The inner compartments of the cell culture inserts were filled with $5 \times 10^4$ PyMT cells in DMEM without FCS. The general cysteine cathepsin inhibitor E64 was added immediately after cell plating (final concentration, 10 μmol/L), and neutralizing cathepsin X antibody (R&D Systems, Minneapolis, MN) at final concentration of 1 μg/mL was preincubated with cells for 15 minutes at 37°C before the assay. The lower compartments were filled with 1 mL DMEM containing 10% FCS as chemoattractant and, where applicable, 10 μmol/L E64 or 1 μg/mL neutralizing cathepsin X antibody. After 20 hours at 37°C and 5% $CO_2$, the inserts were removed, and cells attached to the outside of the porous membrane were obtained by trypsinization and gentle scraping. Vital cells were counted with the CASY cell counter (Schärfe Systems, Reutlingen, Germany).

**Surface labeling of cysteine proteases by active site probes.** Cryopreserved PyMT tumor cells were recultivated for 24 hours, harvested, and counted in a Z1 Series Coulter Cell and Particle Counter (Beckman Coulter, Krefeld, Germany). Cells were plated on six-well plate with $3 \times 10^4/cm^2$ and grown to confluency for another 24 hours. Medium was removed, and cells were incubated for 1 hour at 4°C with ice-cold cell medium containing 50 mmol/L HEPES supplemented with 10 μmol/L DCG-04 non-cell-permeable active site probe (26), specific for labeling of cysteine proteases and containing a biotin tag for recognition by streptavidin. Cells were thoroughly washed and harvested by scraping and lysed on ice in 250 mmol/L Tris-HCl (pH 6.8) and 0.1% Triton X-100 containing 10 mmol/L EDTA for 30 minutes. After clearing by centrifugation at $10,000 \times g$ for 10 minutes at 4°C, the supernatants were used as cell lysates. Protein content was determined with DC Protein Assay (Bio-Rad Laboratories, Inc., Hercules, CA), and lysates were normalized to equal amounts of protein. Proteins were separated by SDS-PAGE, blotted onto a polyvinylidene difluoride (PVDF) membrane, and detected with streptavidin peroxidase. As molecular mass markers, prestained protein standards were used (MBI Fermentas, St. Leon-Rot, Germany).

**Cathepsin X immunolabeling assay.** For immunodetection of cell surface cathepsin X, cysteine proteases were labeled by DCG-04 as described above and purified by use of magnetic beads covalently coupled with streptavidin (Dynabeads M-280 Streptavidin, Dynal, Oslo, Norway). Precipitated surface cysteine proteases were resolved by 15% SDS-PAGE, transferred onto PVDF membranes, and probed with goat anti-cathepsin X antibodies (R&D Systems). Total protein expression of cathepsin X was determined by Western blot of total cell lysate with cathepsin X antibodies and revealed using enhanced chemiluminescence reaction (Pierce, Rockford, IL). Results were normalized to β-actin levels.

**Quantitative real-time PCR.** Total RNA was isolated from PyMT mammary tumors with a RNeasy kit (Qiagen, Valencia, CA). First strand cDNA templates were reversely transcribed from 5 μg total RNA (Invitrogen, Karlsruhe, Germany). Formation of PCR products was measured continuously by SYBR Green incorporation with the iCycler Real-time PCR Detection System (Bio-Rad Laboratories), and the relative amounts of CTSB, cathepsin X, and PyMT mRNA were normalized to the glyceraldehyde-3-phosphate dehydrogenase (GAPDH) transcript. Gene specific primers were as follows: CTSB, 5′-TGCGTTCGGTGAGGACATAG-3′ (forward) and 5′-CGGGCAGTTGGACCATTG-3′ (reverse); cathepsin X, 5′-TATGCCAGCGT-CACCAGGAAC-3′ (forward) and 5′-CCTCTTGATGTTGATTCGGTCTGC-3′(reverse); GAPDH, 5′-TGCACCACCAACTGCTTAG-3′ (forward) and 5′-GATGCAGGGATGATGTTC-3′ (reverse); and PyMT, 5′-CTCCAACAGATA-CACCCGCACATACT-3′ (forward) and 5′-GCTGGTCTTGGTCGCTTT-CTGGATAC-3′ (reverse). For quantification of the PyMT transgene in lung tumor colonies, genomic DNA was isolated from lungs of PyMT cell-recipient mice. Real-time PCR for PyMT and GAPDH quantification was as described above.

**Detection of CTSB enzyme activity.** CTSB proteolytic activity was determined in lysosomal fractions (10 μg protein) in the presence of the fluorogenic substrate Z-Phe-Arg-4-methyl-coumarin-7-amide (20 μmol/L; Bachem, Bubendorf, Switzerland) and in the presence or absence of the

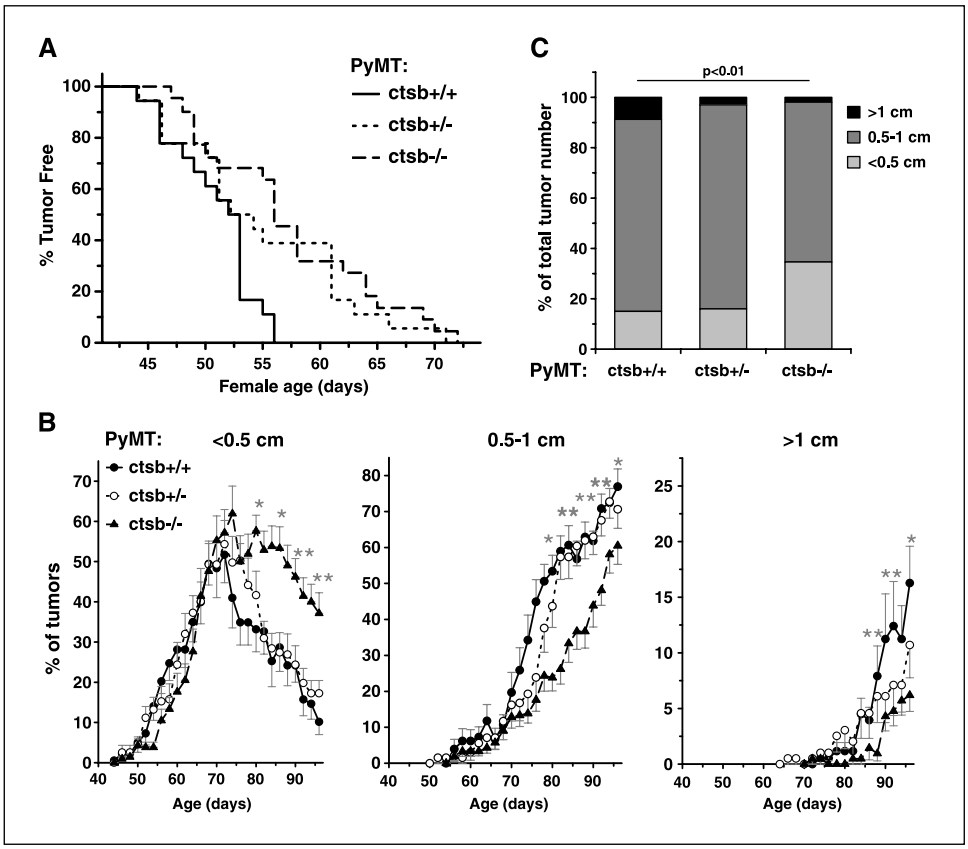


**Figure 1.** Suppression of PyMT-induced tumor growth in CTSB deficient female mice. *A,* Kaplan-Meier plots for tumor-free *PyMT;ctsb*$^{+/+}$ ($n$ = 18), *PyMT;ctsb*$^{+/-}$ ($n$ = 20), and *PyMT;ctsb*$^{-/-}$ ($n$ = 22) female mice. First palpable mammary tumors were detected significantly later in *PyMT;ctsb*$^{-/-}$ female mice than in *PyMT;ctsb*$^{+/+}$ female mice ($P < 0.001$, log-rank test), although the *PyMT;ctsb*$^{+/-}$ showed no significant difference to the other groups. *B,* detailed tumor growth kinetics in *PyMT;ctsb*$^{+/+}$, *PyMT;ctsb*$^{+/-}$, and *PyMT;ctsb*$^{-/-}$ female mice. *Curves,* average number of tumors determined in 2-day intervals according to their diameter of <0.5, 0.5 to 1, and >1 cm. *Asterisks,* statistically significant differences in number of tumors between CTSB knockout and wild-type groups of PyMT transgenic mice, although the *PyMT;ctsb*$^{+/-}$ female mice showed no significant difference to the other groups. *, $P < 0.05$; **, $P < 0.01$, Student's $t$ test. *C,* size of mammary cancer nodes according to their diameter 30 days after the first detection of the individual tumor node. The five mammary tumors that occurred first in each female mouse were analyzed. Thus, 80, 100, and 105 individual tumors were included in the *PyMT;ctsb*$^{+/+}$, *PyMT;ctsb*$^{+/-}$, and *PyMT;ctsb*$^{-/-}$ groups, respectively. The frequencies of tumors according to their diameters were compared between the three CTSB genotypes by $\chi^2$ test.

CTSB-specific inhibitor CA074 (20 nmol/L; Bachem). The release of 7-amino-4-methyl-coumarin was monitored by spectrofluorometry at excitation and emission wavelengths of 360 and 460 nm, respectively.

**Statistical analyses.** Comparisons of arithmetic means between several groups were analyzed by $t$ test (two sided) or ANOVA for experiments with more than two subgroups. *Post hoc* range tests and pair-wise multiple comparisons were done with $t$ test (two sided). Proportions were compared by $\chi^2$ test, and statistical analysis of Kaplan-Meier plots was done by log-rank test. $P \leq 0.05$ was considered as statistically significant. Statistical analyses of lung metastasis were done by analysis of covariance (ANCOVA; Supplementary Data).

## Results

**Progression of PyMT-induced primary carcinomas in female and male mice.** To examine the effect of CTSB on formation of PyMT-induced mammary tumors, *ctsb*$^{-/-}$ mice were bred with transgenic mice predisposed to mammary adenocarcinoma due to expression of the PyMT oncogene in the mammary gland epithelium (23). Female mice, hemizygous for the PyMT transgene, were grouped according to their respective CTSB genotype: (*a*) *PyMT;ctsb*$^{+/+}$, (*b*) *PyMT;ctsb*$^{+/-}$, and (*c*) *PyMT;ctsb*$^{-/-}$. Beginning at age 5 weeks, mice were palpated thrice a week for the development of mammary tumors in a genotype-blinded fashion. No tumors were found in nontransgenic control mice, indicating that the development of the tumor is due to expression of the PyMT transgene. In the female *PyMT;ctsb*$^{-/-}$ group, palpable mammary tumors were detected in all mice at age 72 days, which is 16 days later compared with the control *PyMT;ctsb*$^{+/+}$ mice (Fig. 1*A*). On the average, *PyMT;ctsb*$^{-/-}$ mice possessed a palpable tumor in 1 of their 10 mammary glands by age 57 days, which is ~1 week later than in the *PyMT;ctsb*$^{+/+}$ mice (P < 0.01, log-rank test). After appearance of the first palpable tumor, tumor diameters were measured every 2nd day. We determined that carcinomas developed more slowly in *PyMT;ctsb*$^{-/-}$ mice, which showed tumors in all 10 mammary glands 12 days later than *PyMT;ctsb*$^{+/+}$ (data not shown). However, no statistical significance was observed for the difference of total number of tumors developed by the three groups of PyMT transgenic mice with different genotypes of CTSB (data not shown). To further determine whether the lack of CTSB in PyMT transgenic mice inhibited tumor growth, we divided the tumors according to their size into three groups: <0.5, 0.5 to 1, and >1 cm in diameter (Fig. 1*B*). *PyMT;ctsb*$^{-/-}$ mice developed significantly more small tumors as well as less medium and large size tumors after age 72 days compared with *PyMT;ctsb*$^{+/+}$ and *PyMT;ctsb*$^{+/-}$ mice (Fig. 1*B*). In contrast, *PyMT;ctsb*$^{+/+}$ and *PyMT;ctsb*$^{+/-}$ mice display faster tumor growth with distinctive strong decrease in the number of small tumors after 72 days (Fig. 1*B, right*) and a corresponding increase of medium-sized tumors (Fig. 1*B, middle* and *left*). Figure 1*C* shows the size of tumors according to their diameters 30 days after their first detection. Within these 30 days, significantly less tumors from *PyMT;ctsb*$^{-/-}$ mice developed in medium and large size mammary cancers compared with *PyMT;ctsb*$^{+/+}$, indicating a growth permissive function of CTSB.

In addition, we analyzed the mammary tumor development in *PyMT;ctsb*$^{+/+}$ ($n$ = 15), *PyMT;ctsb*$^{+/-}$ ($n$ = 16), and *PyMT;ctsb*$^{-/-}$ ($n$ = 22) male mice (Supplementary Fig. S1A). The mammary tumor development in male CTSB-deficient tumor mice was even more significantly inhibited compared with *PyMT;ctsb*$^{+/+}$ male mice. Although 50% of *PyMT;ctsb*$^{+/+}$ and *PyMT;ctsb*$^{+/-}$ male mice developed palpable tumors at ages 15 and 18 weeks, respectively,

it took 26 weeks to develop mammary tumors in 50% of *PyMT;ctsb*$^{-/-}$ mice ($P < 0.001$, log-rank test). In contrast to female mice, in which multifocal adenocarcinomas developed in all of the 10 mammary glands, PyMT transgenic male mice on the average developed two mammary tumors without significant difference between the three experimental groups with different CTSB genotypes. Again, the mammary cancers were divided into three groups according to their size at 30 days after the first detection of the tumor (Supplementary Fig. S1B). As the females, male PyMT mice showed significant, genotype-dependent, gradually decreased mammary tumor growth rates in ctsb$^{+/+}$, ctsb$^{-/-}$, and ctsb$^{-/-}$ mice. In contrast to the other genotypes, *PyMT;ctsb*$^{-/-}$ mice did not develop tumors larger than 1 cm in diameter within the 1-month observation period. In summary, these results show increased tumor latency and decreased tumor growth on deletion of CTSB in female and male PyMT mice.

**Pulmonary metastases of PyMT carcinomas and experimental lung colonization by PyMT cancer cells.** A characteristic feature of the MMTV-PyMT adenocarcinoma mouse model is the development of numerous lung metastases that can be observed both macroscopically and microscopically by age 3 to 4 months (23). We estimated the total pulmonary metastases volumes by computer-assisted stereology on systematically sampled histologic lung sections from PyMT female mice of all three experimental groups at age 14 weeks (24). ANCOVA showed that besides genotype (*ctsb*$^{+/+}$, *ctsb*$^{+/-}$, and *ctsb*$^{-/-}$), primary tumor weight, and backcross, generation also had a significant effect on metastasis volume. Furthermore, compared with the *PyMT;ctsb*$^{+/+}$ group, the volume of pulmonary metastases was reduced to 45% in the *PyMT;ctsb*$^{+/-}$ group ($P = 0.01$) and to 65% in the *PyMT;ctsb*$^{-/-}$ group (Fig. 2), although the latter difference in volume of metastatic tumor nodules did not reach statistical significance ($P = 0.13$).

To gain more insight into the role of tumor CTSB in the process of tumor metastasis, we did lung colonization experiments with *LacZ*-tagged primary tumor cells from 98-day-old *PyMT;ctsb*$^{+/+}$, *PyMT;ctsb*$^{+/-}$, and *PyMT;ctsb*$^{-/-}$ female mice. Immunocytochemistry revealed 98% cytokeratin-positive tumor cells in primary cell cultures (data not shown). Adherent *LacZ*-positive tumor cells were injected into the tail vein of congenic female FVB/N recipients. After 21 days, the number of developed lung metastases was determined by counting of LacZ-positive colonies (Supplementary Fig. S2). The number of colonies represents a measure of efficiency of tumor cell seeding and survival in the host tissue. Interestingly, the injection of *PyMT;ctsb*$^{+/-}$ cells resulted in significantly reduced number of lung colonies compared with *PyMT;ctsb*$^{+/+}$, an effect that was not further enhanced for the *PyMT;ctsb*$^{-/-}$ cells (Fig. 3*A*). As a further measure of efficiency of metastasis, the amount of the PyMT transgene in genomic DNA from lungs of animals after PyMT cell injection was quantified and divided by the number of lung tumor nodules present in the individual mouse (Fig. 3*B*). For the *PyMT;ctsb*$^{+/-}$ and *PyMT;ctsb*$^{-/-}$ cells, the assay revealed a 90% reduction of lung colony size compared with the *PyMT;ctsb*$^{+/+}$ group (Fig. 3*B*). Thus cancer

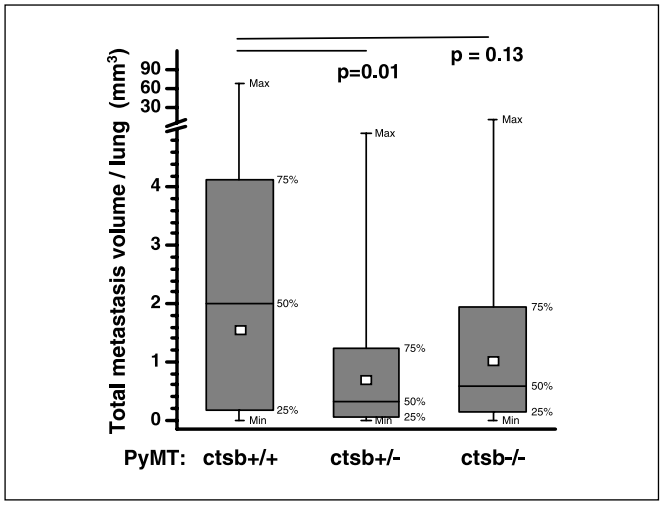


**Figure 2.** Effect of CTSB deficiency on pulmonary metastases of PyMT mammary tumors. Histomorphometric determination of lung metastasis volumes in *PyMT;ctsb*$^{+/+}$ ($n = 36$), *PyMT;ctsb*$^{+/-}$ ($n = 38$), and *PyMT;ctsb*$^{-/-}$ ($n = 32$) female mice at age 14 weeks. *Boxes,* values between the 25th and 75th percentile; *squares,* adjusted mean obtained by ANCOVA (see Materials and Methods). *Bars,* minimum and maximum values.

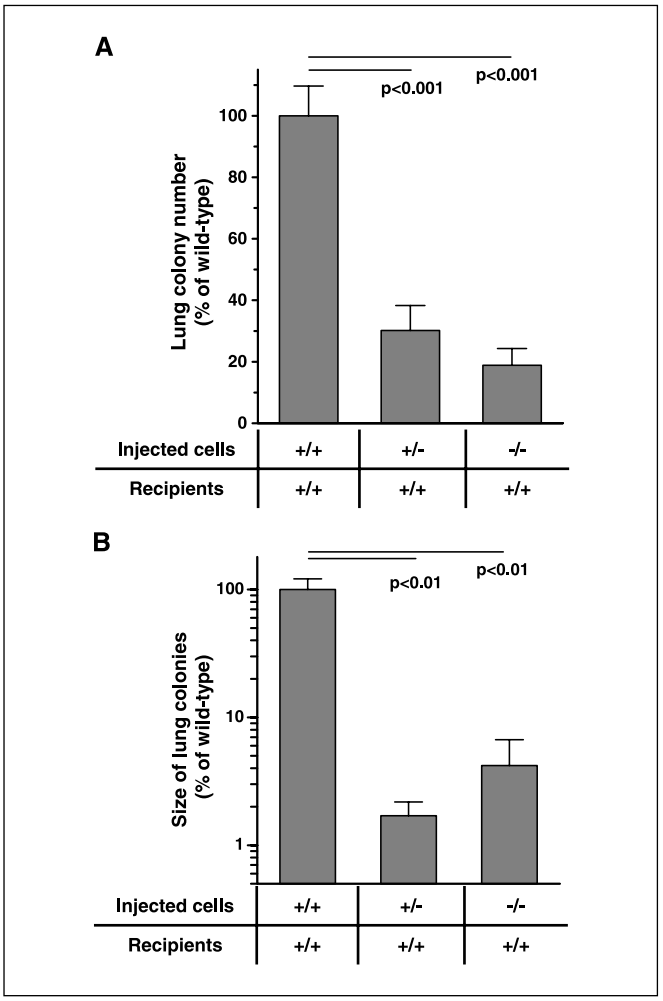


**Figure 3.** Lung colonization by i.v. injected PyMT cells of varying CTSB genotype into congenic wild-type recipients. Number of lung colonies (*A*) and average volume of tumor colonies in lung tissue (*B*) after injection of primary *PyMT;ctsb*$^{+/+}$, *PyMT;ctsb*$^{+/-}$, and *PyMT;ctsb*$^{-/-}$ tumor cells. The total volume of lung colonies was measured by real-time PCR quantification of the PyMT transgene in genomic lung DNA normalized to the *GAPDH* gene. The amount of *PyMT* gene divided by the number of tumor colonies gives a measure of the average volume of PyMT cell-derived tumor nodules in an individual mouse. *Columns,* mean; *bars,* SE. Significance levels were calculated by *t* test.

cell–derived CTSB promotes both seeding and growth of experimental metastases.

**Cell surface cathepsin X compensates for CTSB in *PyMT;ctsb*$^{-/-}$ tumor cells.** To further investigate the effects of CTSB in primary and experimental lung metastasis, we studied primary PyMT tumor cells in cell culture. First, we examined the gene expression and activity of CTSB in tumor cells by quantitative reverse transcription-PCR and degradation of a fluorogenic CTSB peptide substrate, respectively (Fig. 4*A*). Tumor cells isolated from *PyMT;ctsb*$^{+/-}$ mice showed 30% reduced CTSB expression and CTSB activity compared with *PyMT;ctsb*$^{+/+}$ cells, and neither CTSB mRNA nor activity was detectable in *PyMT;ctsb*$^{-/-}$ tumor cells. Viability, growth, and proliferation rate of tumor cells were not affected by the CTSB genotypes (Fig. 4*B*). Consistent with the *in vivo* findings in metastasis of primary PyMT carcinomas and experimental lung colonization, significantly reduced of invasion across Matrigel-occluded porous membranes was seen in tumor cells heterozygous for CTSB, whereas deletion of the second CTSB allele did not result in additional reduction of invasion (Fig. 4*C*). Notably, after treating the cells with the membrane-impermeable, broad-spectrum inhibitor of cysteine proteases E64, the Matrigel invasion of PyMT tumor cells was decreased to baseline levels in all three tumor cell types with different CTSB genotypes (Fig. 4*C*). This result suggests a compensation for loss of CTSB by other cysteine protease/s that are sensitive to E64.

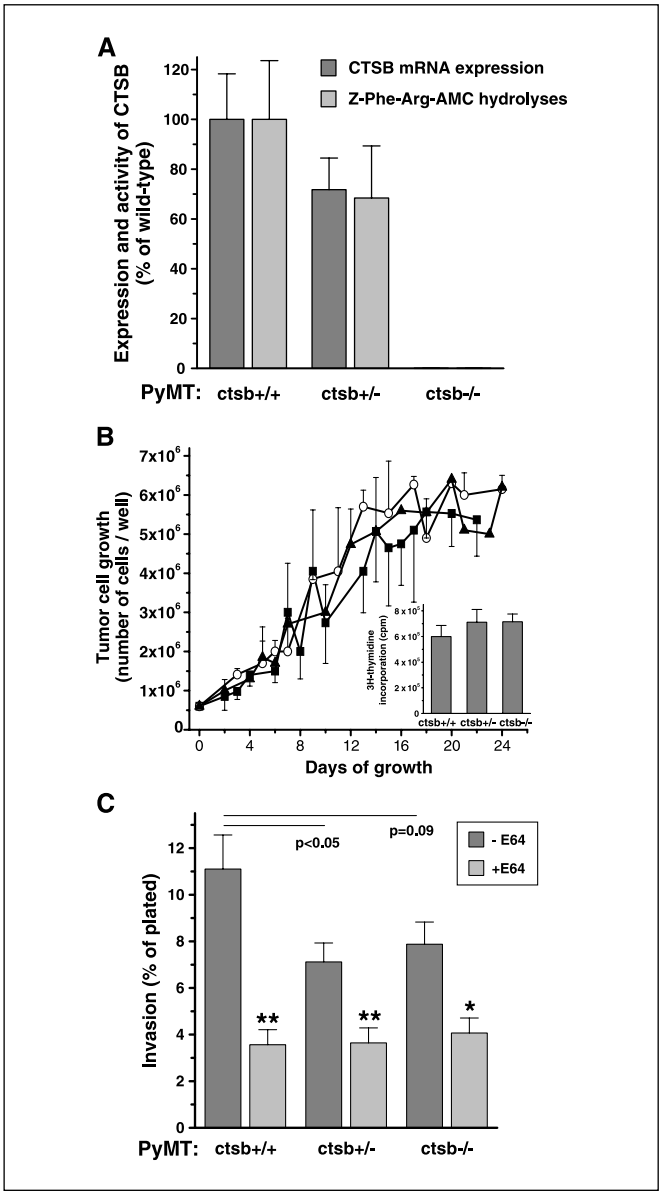


**Figure 4.** *In vitro* analyses of tumor cells prepared from PyMT-induced carcinomas. *A,* CTSB mRNA expression and activity in *PyMT;ctsb*$^{+/+}$, *PyMT;ctsb*$^{+/-}$, and *PyMT;ctsb*$^{-/-}$ tumor cells. CTSB mRNA was quantified by real-time PCR and normalized to GAPDH expression. Activity was measured as Z-Phe-Arg-AMC hydrolysis that is sensitive to the CTSB-specific inhibitor CA-074 ($n = 3$). *B, in vitro* growth curves of tumor cells from *PyMT;ctsb*$^{+/+}$ (■, $n = 3$), *PyMT;ctsb*$^{+/-}$ (○, $n = 4$), and *PyMT;ctsb*$^{-/-}$ (▲; $n = 5$) tumor mice. *Inset,* proliferation measurement by 3H-thymidine incorporation into DNA of PyMT cells after a culture period of 5 days ($n = 3$). *C,* Matrigel invasion of tumor cells in the presence and absence of the cysteine protease inhibitor E64 (**, $P < 0.01$; *, $P < 0.05$ for E64 treated versus untreated, *t* test; $n = 3$). *Columns,* mean; *bars,* SE.

Based on the assumption that most of the protease activity required for tumor cell invasion is supplied by extracellularly exposed proteases, we determined the activity profiles of cysteine cathepsins at the cell surface of PyMT cells (Fig. 5*A*). Cell surface labeling of active cysteine cathepsins with the membrane-impermeable active site probe DCG-04 (26) revealed the presence of cell surface-associated CTSB in *PyMT;ctsb*$^{+/+}$ and *PyMT;ctsb*$^{+/-}$ cells, although CTSB was not detectable on *PyMT;ctsb*$^{-/-}$ cells (Fig. 5*A*). Interestingly, overexpression of distinct cysteine protease bands was detected at the surface of CTSB-deficient tumor cells (Fig. 5*A*). The major up-regulated band detected at the surface of *PyMT;ctsb*$^{-/-}$ cells comigrated in the SDS-PAGE with the cysteine protease cathepsin X (alternative names: cathepsin Z; cathepsin P) as detected by Western blotting (Fig. 5*A*). Precipitation of DCG-04-labeled proteases via its biotin tag and subsequent immunoblotting further confirmed the identification of the up-regulated cell surface cysteine protease cathepsin X (Fig. 5*B*). To assess the contribution of cathepsin X for invasion of PyMT tumor cells, a neutralizing anti-cathepsin X antibody, specifically inhibiting cathepsin X, has been used for Matrigel assays (Fig. 5*C*). In an initial experiment, several antibody concentrations in the range of 0.01 to 10 μg/mL were tested in Matrigel assays with *PyMT;ctsb*$^{-/-}$ cells, and the antibody concentration of 1 μg/mL was found to result in 40% inhibition of invasion, an effect that was not further enhanced by higher amounts of antibody (data not shown). Remarkably, neutralizing anti-cathepsin X antibody treatment significantly reduced Matrigel invasion of *PyMT;ctsb*$^{-/-}$ cells but did not affect invasion of *PyMT;ctsb*$^{+/+}$ or *PyMT;ctsb*$^{+/-}$ cells (Fig. 5*C*). To further determine whether cathepsin X is up-regulated at the transcriptional or post-translational level, the expression of cathepsin X was measured by quantitative real-time PCR (data not shown), and the protein amount was determined by Western blot of total cell extract (Fig. 5*D*). No significant difference in cathepsin X mRNA or protein expression was found in the tumor cells with different CTSB genotypes, suggesting that enhanced surface activity of cathepsin X results from the redistribution of the enzyme to the cell surface. Thus, these results indicate that the absence of CTSB in PyMT tumor cells induces an increase of extracellular cathepsin X activity via its recruitment to the cell surface, compensating at least partially for the CTSB deficiency.

**Host effects on lung colonization by PyMT tumor cells.** CTSB in a tumor can be either derived from the tumor cells or expressed by cells of the tumor stroma. Recent studies have suggested a role for non-tumor-derived proteases in promotion of tumor growth

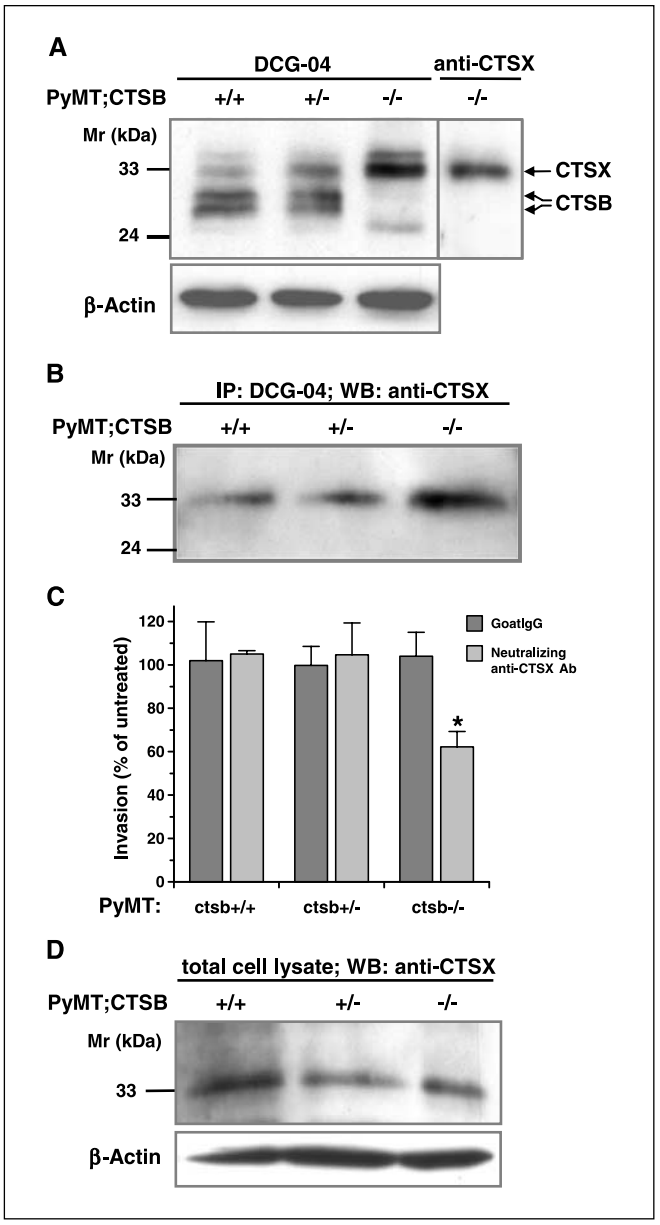


**Figure 5.** Expression pattern of active cysteine cathepsins on the surface of PyMT tumor cells. *A,* cell surface labeling of cysteine protease by the active site probe DCG-04. PyMT tumor cells were incubated with 10 μmol/L DCG-04 for 1 hour at 4°C and PBS washed. Western blots of cell lysates were developed with streptavidin peroxidase. Representative blot of four independent experiments. β-Actin serves as a loading control. *B,* identification of cell surface cathepsin X in PyMT tumor cells. Cathepsin X on the plasma membrane of PyMT tumor cells was revealed by precipitation of cell surface DCG-04-labeled cysteine proteases by streptavidin-coupled beads followed by Western blot detection with anti-cathepsin X antibody. *C,* effect of neutralizing anti-cathepsin X antibody on Matrigel invasion by PyMT tumor cells (*, $P < 0.05$ for *PyMT;ctsb*$^{-/-}$ tumor cells versus *PyMT;ctsb*$^{+/+}$ tumor cells, *t* test; $n = 3$). Cells were incubated for 24 hours in the presence of cathepsin X neutralizing antibody or control goat IgG, all at 1 μg/mL concentration. Matrigel invasion is expressed as a percentage of inhibition of invasion relative to each individual untreated control. *Columns,* mean; *bars,* SE. *D,* cathepsin X analyzed by immunoblotting in total cell lysate of (*A*). *B* and *C,* representative for three independent experiments. β-Actin serves as a loading control. Molecular mass markers are given in the left margin.

and metastasis (21, 27). To explore the possible functional role of CTSB derived from the tumor microenvironment, we i.v. injected four different *LacZ*-tagged *PyMT;ctsb*$^{+/+}$ primary tumor cell lines, each isolated from individual primary PyMT tumors, into congenic *ctsb*$^{+/+}$, *ctsb*$^{+/-}$, and *ctsb*$^{-/-}$ female mice that did not carry the PyMT transgene. These studies revealed that the complete loss of CTSB expression in recipient mice resulted in 50% reduction of pulmonary tumor colony number relative to *ctsb*$^{+/+}$ and *ctsb*$^{+/-}$ recipients (Fig. 6*A*). In addition, the average volume of nodules in the lungs of *ctsb*$^{-/-}$ recipients was reduced by 90% compared with the *ctsb*$^{+/+}$ and *ctsb*$^{+/-}$ recipients (Fig. 6*B*). Subsequently, CTSB expression in PyMT lung colonies was investigated by immunohistochemistry to more precisely determine the source of CTSB within developing tumors (Supplementary Fig. S3). As expected, tumor colonies derived from *PyMT;ctsb*$^{+/+}$ tumor cells injected to *ctsb*$^{+/+}$ showed strong CTSB expression throughout the tumor mass. Similarly, *PyMT;ctsb*$^{-/-}$ tumor cells injected into *ctsb*$^{-/-}$ recipients showed no staining for CTSB. The majority of CTSB expression in lung colonies was derived from the *PyMT;ctsb*$^{+/+}$ tumor cells injected into *ctsb*$^{-/-}$ recipients. Interestingly, when *PyMT;ctsb*$^{-/-}$ cells were injected into *ctsb*$^{+/+}$ recipients, a strong CTSB staining was found in several distinct cells, mainly located near the edge of the lung colony. Pervious work has shown that lung metastasis formation in the MMTV-PyMT breast cancer model positively correlates with the extent of macrophage recruitment to the tumor (28). Therefore, double immunofluorescence was done for macrophages (antibody F4/80) and CTSB (Fig. 6*C*). Tumor colonies produced by *PyMT;ctsb*$^{-/-}$ cells injected into *ctsb*$^{+/+}$ recipient mice showed an infiltration by macrophages with high expression of CTSB (Fig. 6*C, yellow*). In contrast, macrophages distant from the tumor colony did not show any considerable expression of CTSB (Fig. 6*C, red*). These data suggest that macrophages up-regulate CTSB expression on being recruited to the tumor node and that macrophage-derived CTSB promotes growth of PyMT colonies in the lung.

## Discussion

During progression to high malignancy, tumor cells acquire multiple mutations that affect proliferation, programmed death, and genetic stability (29). Furthermore, a favorable microenvironment is essential for growth, invasion, and metastasis of a tumor (1). Proteases capable of degrading ECM proteins have recently been identified as critical regulators of the tumor microenvironment. Here, we show that the lysosomal cysteine protease CTSB contributes to growth, invasion, and metastatic process of PyMT-induced mammary carcinoma.

CTSB is overexpressed and also secreted by malignant cells and, in some studies, was found to be secreted from stromal cells closely associated with the tumor (12, 13). Mature CTSB, as well as the proteolytically inactive proenzyme, was detected in soluble form within the extracellular space and also found to be associated with the plasma membrane (30–32). These observations are consistent with our findings for cell surface expression of CTSB in PyMT mouse mammary cancer cells. Labeling with the broad-spectrum cathepsin probe DCG-04 revealed that CTSB is the most active cysteine cathepsin on the cell surface of wild-type PyMT cells. Cell surface association of CTSB can be achieved through an interaction with Annexin II heterotetramers that direct CTSB to caveolae (33). Furthermore, CTSB exerts proteolytic activity at the cell surface at neutral or slightly acidic pH (34) and can initiate proteolytic cascades through activation of MMP (e.g., MMP-3) and/or urokinase-type plasminogen activator and is capable of degrading the ECM proteins laminin, type IV collagen, and fibronectin (35). Accordingly, CTSB inhibition by synthetic inhibitors, antibodies,

or antisense RNA clearly reduces tumor cell migration and invasion into ECM-like matrices *in vitro* (18, 19), whereas CTSB overexpression facilitates these processes (20, 36). These potential roles for CTSB in tumor cells are supported by our analysis of the PyMT mammary cancer model crossed with CTSB-deficient mice. Female and male mice exhibit a CTSB genotype-correlated delay in development of palpable tumors and reduced tumor growth rates, but absolute tumor numbers are not altered by the CTSB genotype. This clearly indicates that CTSB is not critical for tumorigenic transformation of selected cell clones but rather contributes to overcoming tumor cell dormancy by promoting invasive growth, a process that occurs most likely by degradation of the ECM.

Tumor cell metastasis is a complex cascade of sequential steps, in which tumor cells disseminate, extravasate from the vessel, invade new tissue, and proliferate to produce metastatic foci (37). CTSB expression on the gene and protein level has been correlated with metastasis (38, 39); however, little is known about the functional relevance of CTSB for the metastatic process *in vivo*. In the present study, the role of cancer cell–derived CTSB has been addressed by analysis of spontaneous pulmonary metastases as well as lung metastases, resulting from introduction of primary PyMT cells of different CTSB genotypes and *ex vivo* migration/invasion of isolated PyMT tumor cells. Taken together, these experiments clearly indicate that CTSB contributes to metastasis in the PyMT mammary cancer model. The reduced migration and invasion of tumor cells with reduced CTSB levels *in vitro* provides circumstantial evidence for a contribution of CTSB to tumor cell dissemination from primary tumors. More directly, the lung colonization experiments revealed that CTSB supports the sequestration of PyMT cells into the lung tissue because a lower number of tumor nodules were present in lungs after injection of *PyMT;ctsb*$^{+/-}$ and *PyMT;ctsb*$^{-/-}$ cells. In addition, our results

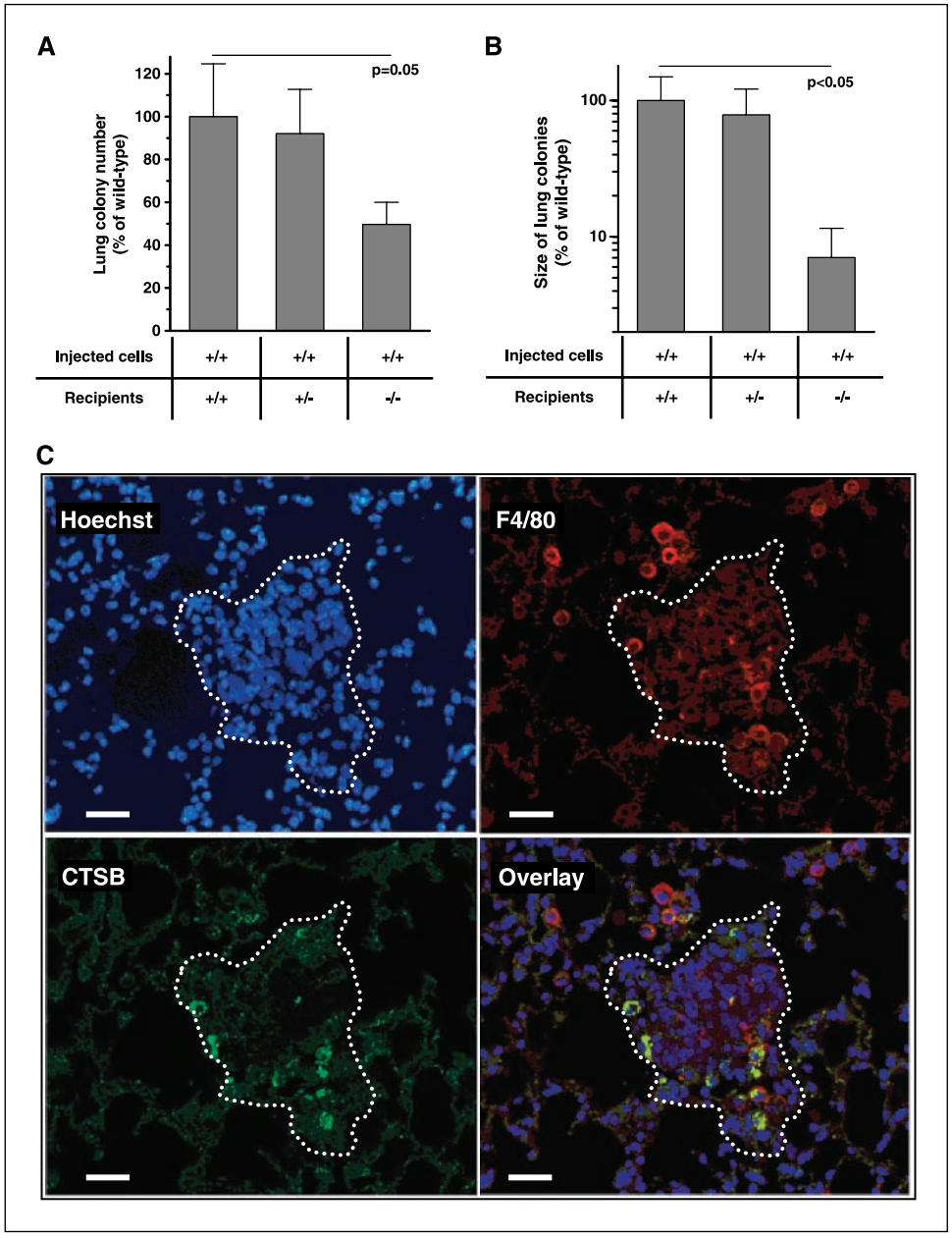


**Figure 6.** Effect of host-derived CTSB on lung colonization of PyMT cells. Number of lung colonies (*A*) and average volume of tumor colonies in lung tissue (*B*) after i.v. injection of LacZ-marked *PyMT;ctsb*$^{+/+}$ cells into congenic *ctsb*$^{+/+}$, *ctsb*$^{+/-}$, and *ctsb*$^{-/-}$ recipient mice at 21 days after injection. Colony number was determined by counting the blue, LacZ-positive tumor nodules in the lung. The total volume of lung colonies was measured by real-time PCR quantification of the PyMT transgene in genomic lung DNA normalized to the *GAPDH* gene. The amount of *PyMT* gene divided by the number of tumor colonies gives a measure of the average volume of PyMT cell-derived tumor nodules in an individual mouse. Four independently isolated *PyMT;ctsb*$^{+/+}$ cancer cell preparations were marked by LacZ and subsequently injected in five mice per cell preparation. *C,* induction of CTSB expression in tumor-associated macrophages. CTSB-deficient PyMT tumor cells were i.v. injected into a congenic wild-type recipient mouse. *Dotted lines,* resulting lung tumor colony. *Blue,* Hoechst 33342 nuclear staining; *red,* F4/80 staining of macrophages; *green,* CTSB detection; *yellow,* cells coexpressing F4/80 and CTSB. Notably, CTSB expression is not detectable in macrophages distant from the tumor, whereas tumor-associated macrophages show strong CTSB fluorescence. Bar, 50 μm.

suggest that CTSB is also involved in the support of growth of tumor colonies because the volume of lung nodules derived from *PyMT;ctsb*$^{+/-}$ and *PyMT;ctsb*$^{-/-}$ cells was highly reduced. A remarkable and unexpected finding in all of these experiments was the strong reduction of metastasis burden, lung colony formation, and Matrigel invasion in *ctsb*$^{+/-}$ PyMT tumors or isolated PyMT tumor cells derived from *PyMT;ctsb*$^{+/-}$ mice. Remarkably, these effects were not enhanced by total ablation of CTSB expression in the homozygous knockout groups. In an attempt to understand these results, we probed the surface of primary PyMT cells for active cysteine cathepsins using a broad-spectrum activity-based probe. *PyMT;ctsb*$^{-/-}$ cells showed a redistribution of active cathepsin X to the cell surface, resulting in at least a partial compensation for loss of CTSB function as shown by reduction of tumor cell invasion on treatment of CTSB-deficient cells with a neutralizing cathepsin X antibody. Cathepsin X is a recently discovered cysteine protease that is up-regulated in human cancers (40, 41). Strikingly, cathepsin X and CTSB are the only carboxypeptidase enzymes in the cysteine cathepsin family, although CTSB exhibits an additional endopeptidase activity (42, 43). This suggests that cathepsin carboxypeptidase activity contributes significantly to invasion.

High levels of CTSB have frequently been detected at the invasive edge of tumors (13, 14, 44). The cellular source of this protease in solid tumors, consisting of both malignant tumor cells and a variety of stromal cells (e.g., fibroblasts, endothelial cells, and bone marrow–derived inflammatory cells), has remained elusive. CTSB has been reported to be expressed in stromal fibroblasts and macrophages in carcinomas of breast, colon, and prostate (14, 45, 46); however, the specific contribution of CTSB from these cell populations to tumor cell growth and invasiveness has not yet been defined. Here, we do lung colonization experiments with PyMT cancer cells i.v. injected into *ctsb*$^{+/+}$, *ctsb*$^{+/-}$, and *ctsb*$^{-/-}$ recipient mice. Interestingly, CTSB deficiency of the recipient resulted in reduced seeding efficiency. However, the size reduction of tumor nodules was even more significant in the *ctsb*$^{-/-}$ recipients, indicating that host cell–derived CTSB is potentially as important as tumor-derived protease activity for metastatic growth. In the search for host cells that supply CTSB, we identified tumor-infiltrating macrophages, which induce CTSB expression on entry into the tumor mass. This result is in line with a recent report suggesting that macrophages contribute to the development of invasive, metastatic carcinomas in the MMTV-PyMT mammary cancer model (28). This intriguing role of tumor-associated macrophages was recently suggested to be of general significance in the progression of solid tumors (47). In addition to CTSB, macrophages may produce other proteases (e.g., MMP-9) that contributes to carcinogenesis in mice (27). Thus, our present data provide further evidence for functional involvement of proteolytic enzymes of tumor-invading bone marrow–derived cells in cancer progression (48).

In summary, the present results suggest that CTSB derived from both tumor and stromal cells from the microenvironment plays critical roles in multiple stages of tumor growth and metastasis. Thus, pharmacologic inhibition of extracellular CTSB within and around a tumor by plasma membrane-impermeable inhibitors may be a promising route for effective cancer treatment.

## Acknowledgments

Received 12/14/2005; revised 2/16/2006; accepted 3/13/2006.

**Grant support:** Deutsche Forschungsgemeinschaft (SFB 364; B12) grant 23-7532.22-33-11/1 of the Ministerium für Wissenschaft und Kunst, Baden-Wuerttemberg, and the European Union Framework Programme 6, Project LSHC-CT-2003-503297, Cancerdegradome (A. Krüger).

The costs of publication of this article were defrayed in part by the payment of page charges. This article must therefore be hereby marked *advertisement* in accordance with 18 U.S.C. Section 1734 solely to indicate this fact.

We thank Susanne Dollwet-Mack, Anne Schwinde, and Ulrike Stabenow (Institut für Molekulare Medizin und Zellforschung, Freiburg, Germany) and Katja Honert (Institut für Experimentelle Onkologie, Munich, Germany) for excellent technical assistance.

## References

1. Liotta LA, Kohn EC. The microenvironment of the tumour-host interface. Nature 2001;411:375–9.
2. Del Rosso M, Fibbi G, Pucci M, et al. Multiple pathways of cell invasion are regulated by multiple families of serine proteases. Clin Exp Metastasis 2002;19:193–207.
3. Egeblad M, Werb Z. New functions for the matrix metalloproteinases in cancer progression. Nat Rev Cancer 2002;2:161–74.
4. Turk V, Kos J, Turk B. Cysteine cathepsins (proteases)—on the main stage of cancer? Cancer Cell 2004;5:409–10.
5. Rawlings ND, Barrett AJ. MEROPS: the peptidase database. Nucleic Acids Res 2000;28:323–5.
6. Deussing J, Kouadio M, Rehman S, et al. Identification and characterization of a dense cluster of placenta-specific cysteine peptidase genes and related genes on mouse chromosome 13. Genomics 2002;79:225–40.
7. Barrett AJ. Cellular proteolysis. An overview. Ann N Y Acad Sci 1992;674:1–15.
8. Nakagawa T, Roth W, Wong P, et al. Cathepsin L: critical role in Ii degradation and CD4 T cell selection in the thymus. Science 1998;280:450–3.
9. Friedrichs B, Tepel C, Reinheckel T, et al. Thyroid functions of mouse cathepsins B, K, and L. J Clin Invest 2003;111:1733–45.
10. Yasothornsrikul S, Greenbaum D, Medzihradszky KF, et al. Cathepsin L in secretory vesicles functions as a prohormone-processing enzyme for production of the enkephalin peptide neurotransmitter. Proc Natl Acad Sci U S A 2003;100:9590–5.
11. Goulet B, Baruch A, Moon NS, et al. A cathepsin L isoform that is devoid of a signal peptide localizes to the nucleus in S phase and processes the CDP/Cux transcription factor. Mol Cell 2004;14:207–19.
12. Sloane BF, Yan S, Podgorski I, et al. Cathepsin B and tumor proteolysis: contribution of the tumor microenvironment. Semin Cancer Biol 2005;15:149–57.
13. Poole AR, Tiltman KJ, Recklies AD, Stoker TA. Differences in secretion of the proteinase cathepsin B at the edges of human breast carcinomas and fibroadenomas. Nature 1978;273:545–7.
14. Castiglioni T, Merino MJ, Elsner B, Lah TT, Sloane BF, Emmert-Buck MR. Immunohistochemical analysis of cathepsins D, B, and L in human breast cancer. Hum Pathol 1994;25:857–62.
15. Saad Z, Bramwell VH, Wilson SM, O'Malley FP, Jeacock J, Chambers AF. Expression of genes that contribute to proliferative and metastatic ability in breast cancer resected during various menstrual phases. Lancet 1998;351:1170–3.
16. Frohlich E, Schlagenhauff B, Mohrle M, Weber E, Klessen C, Rassner G. Activity, expression, and transcription rate of the cathepsins B, D, H, and L in cutaneous malignant melanoma. Cancer 2001;91:972–82.
17. Staack A, Koenig F, Daniltchenko D, et al. Cathepsins B, H, and L activities in urine of patients with transitional cell carcinoma of the bladder. Urology 2002;59:308–12.
18. Premzl A, Zavasnik-Bergant V, Turk V, Kos J. Intracellular and extracellular cathepsin B facilitate invasion of MCF-10A neoT cells through reconstituted extracellular matrix *in vitro*. Exp Cell Res 2003;283:206–14.
19. Mohanam S, Jasti SL, Kondraganti SR, et al. Down-regulation of cathepsin B expression impairs the invasive and tumorigenic potential of human glioblastoma cells. Oncogene 2001;20:3665–73.
20. Coulibaly S, Schwihla H, Abrahamson M, et al. Modulation of invasive properties of murine squamous carcinoma cells by heterologous expression of cathepsin B and cystatin C. Int J Cancer 1999;83:526–31.
21. Joyce JA, Baruch A, Chehade K, et al. Cathepsin cysteine proteases are effectors of invasive growth and angiogenesis during multistage tumorigenesis. Cancer Cell 2004;5:443–53.
22. Halangk W, Lerch MM, Brandt-Nedelev B, et al. Role of cathepsin B in intracellular trypsinogen activation and the onset of acute pancreatitis. J Clin Invest 2000;106:773–81.
23. Guy CT, Cardiff RD, Muller WJ. Induction of mammary tumors by expression of polyomavirus middle T oncogene: a transgenic mouse model for metastatic disease. Mol Cell Biol 1992;12:954–61.
24. Nielsen BS, Lund LR, Christensen IJ, et al. A precise and efficient stereological method for determining murine lung metastasis volumes. Am J Pathol 2001;158:1997–2003.
25. Krüger A, Schirrmacher V, von Hoegen P. Scattered

micrometastases visualized at the single-cell level: detection and re-isolation of lacZ-labeled metastasized lymphoma cells. Int J Cancer 1994;58:275–84.
**26.** Greenbaum D, Medzihradszky KF, Burlingame A, Bogyo M. Epoxide electrophiles as activity-dependent cysteine protease profiling and discovery tools. Chem Biol 2000;7:569–81.
**27.** Coussens LM, Tinkle CL, Hanahan D, Werb Z. MMP-9 supplied by bone marrow-derived cells contributes to skin carcinogenesis. Cell 2000;103:481–90.
**28.** Lin EY, Nguyen AV, Russell RG, Pollard JW. Colony-stimulating factor 1 promotes progression of mammary tumors to malignancy. J Exp Med 2001;193:727–40.
**29.** Hanahan D, Weinberg RA. The hallmarks of cancer. Cell 2000;100:57–70.
**30.** Rozhin J, Sameni M, Ziegler G, Sloane BF. Pericellular pH affects distribution and secretion of cathepsin B in malignant cells. Cancer Res 1994;54:6517–25.
**31.** Arkona C, Wiederanders B. Expression, subcellular distribution, and plasma membrane binding of cathepsin B and gelatinases in bone metastatic tissue. Biol Chem 1996;377:695–702.
**32.** Mai J, Finley RL, Waisman DM, Sloane BF. Human procathepsin B interacts with the annexin II tetramer on the surface of tumor cells. J Biol Chem 2000;275:12806–12.
**33.** Cavallo-Medved D, Dosescu J, Linebaugh BE, Sameni M, Rudy D, Sloane BF. Mutant K-*ras* regulates cathepsin B localization in caveolae of human colorectal carcinoma cells. Neoplasia 2003;5:507–19.
**34.** Linebaugh BE, Sameni M, Day NA, Sloane BF, Keppler D. Exocytosis of active cathepsin B enzyme activity at pH 7.0, inhibition, and molecular mass. Eur J Biochem 1999;264:100–9.
**35.** Skrzydlewska E, Sulkowska M, Koda M, Sulkowski S. Proteolytic-antiproteolytic balance and its regulation in carcinogenesis. World J Gastroenterol 2005;11:1251–66.
**36.** Szpaderska AM, Frankfater A. An intracellular form of cathepsin B contributes to invasiveness in cancer. Cancer Res 2001;61:3493–500.
**37.** Chambers AF, Groom AC, MacDonald IC. Dissemination and growth of cancer cells in metastatic sites. Nat Rev Cancer 2002;2:563–72.
**38.** Nagai A, Terashima M, Harada T, et al. Cathepsin B and H activities and cystatin C concentrations in cerebrospinal fluid from patients with leptomeningeal metastasis. Clin Chim Acta 2003;329:53–60.
**39.** Tzanakakis GN, Margioris AN, Tsatsakis AM, Vezeridis MP. The metastatic potential of human pancreatic cell lines in the liver of nude mice correlates well with cathepsin B activity. Int J Gastrointest Cancer 2003;34:27–38.
**40.** Nägler DK, Krüger S, Kellner A, et al. Up-regulation of cathepsin X in prostate cancer and prostatic intraepithelial neoplasia. Prostate 2004;60:109–19.
**41.** Krüger S, Kalinski T, Hundertmark T, et al. Up-regulation of cathepsin X in Helicobacter pylori gastritis and gastric cancer. J Pathol 2005;207:32–42.
**42.** Nägler DK, Zhang R, Tam W, Sulea T, Purisima EO, Menard R. Human cathepsin X: a cysteine protease with unique carboxypeptidase activity. Biochemistry 1999;38:12648–54.
**43.** Klemencic I, Carmona AK, Cezari MH, et al. Biochemical characterization of human cathepsin X revealed that the enzyme is an exopeptidase, acting as carboxymonopeptidase or carboxydipeptidase. Eur J Biochem 2000;267:5404–12.
**44.** Emmert-Buck MR, Roth MJ, Zhuang Z, et al. Increased gelatinase A (MMP-2) and cathepsin B activity in invasive tumor regions of human colon cancer samples. Am J Pathol 1994;145:1285–90.
**45.** Campo E, Munoz J, Miquel R, et al. Cathepsin B expression in colorectal carcinomas correlates with tumor progression and shortened patient survival. Am J Pathol 1994;145:301–9.
**46.** Fernandez PL, Farre X, Nadal A, et al. Expression of cathepsins B and S in the progression of prostate carcinoma. Int J Cancer 2001;95:51–5.
**47.** Pollard JW. Opinion: Tumour-educated macrophages promote tumour progression and metastasis. Nat Rev Cancer 2004;4:71–8.
**48.** Coussens LM, Werb Z. Inflammation and cancer. Nature 2002;420:860–7.